Journal of Building Engineering 44 (2021) 103381

Contents lists available at ScienceDirect

Journal of Building Engineering

journal homepage: www.elsevier.com/locate/jobe

Analysis of the materials and state of conservation of the medieval rammed earth walls of Seville (Spain)

J.J. Martín-del-Rio [a,*], J. Canivell [a], Marta Torres-González [a,b], E.J. Mascort-Albea [c], R. Romero-Hernández [c], J.M. Alducin-Ochoa [a], F.J. Alejandre-Sánchez [a]

[a] Department of Architectural Construction II, Universidad de Sevilla, Spain
[b] Department of Civil Engineering, Architecture and Georesources, University of Lisbon, Portugal
[c] Department of Building Structures and Soil Engineering, Universidad de Sevilla, Spain

ARTICLE INFO

Keywords:
Rammed earth
Fortifications
Chemical & mineralogical analysis
Physical & mechanical properties
Architectural heritage

ABSTRACT

In the specific study of medieval fortifications, an advanced knowledge of the state of conservation is required to achieve an effective diagnosis and a detailed evaluation that will provide the basis for establishing the criteria for prevention and restoration. The characterization of the materials and the knowledge of their degree of deterioration is one of the key points to address a restoration project in any rammed earth wall. In the last decades, a number of medieval fortifications built with rammed earth in Spain have been studied and restored. Although there is currently a better knowledge of the construction materials involved and their degradation processes, no detailed work has been carried out to date on the Seville City Wall, which is an outstanding sample of this kind of heritage. The aim of this work is hence to study the material characterization of the most recognisable section of the whole structure, which is known as Macarena Wall, that runs between the Macarena and the Cordoba Gates. The results and discussions presented offer a novel approach for this heritage asset and would play a solid criterion for a correct restoration proposal. For this purpose, ananalytical methodology already known and verified in the literature has been followed, which has been adapted according to the specific requirements of this monumental building. Among the most relevant results of the analytical and experimental phase, it is highlighted that capillary humidity and the transport and crystallisation of salts is one of the main causes of the deterioration of this monument. As this building is a clear reference of rammed earth military structures, the analytical procedure and the results obtained are an interesting reference for other similar interventions.

1. Introduction

Earth can be used as a building material for the development of different construction systems, although it is mainly focused on walls. This resource has been documented in historical sites [1] and nowadays, thanks to its environmental benefits, it has been the topic of a great diversity of scientific studies [2]. When the earth is compacted within reusable formworks and its water content is lower than plastic limit, it is called “rammed earth”.

In its traditional version, the walls usually reach a thickness between 50 and 60 cm, which are executed in units called boxes of 200 cm long and 90 cm high. The horizontal succession of boxes forms a course, which, once hardened, allows another course to be overlapped until the wall is finished [3,4]. When it comes to more massive construction systems, as in the case of military architecture, the technique is adapted by changing the auxiliary means (formwork system) and the type of materials used. These military walls, for instance, may reach thicknesses of more than 150 cm, although the module of the lift is usually the same. Both cases, traditional and military rammed earth walls, have been analysed by López Martínez [5].

The present study will be focused on the historical military structures of the Iberian Peninsula, and specifically in the city of Sevilla, where the use of this type of walls became extensive during the period of Almohad rule (12th-13th centuries AD). In this context, construction techniques have been studied by various authors from a general perspective [6,7] to specific cases [8–10] or even concerning their historical evolution [11, 12].

From a methodological perspective, there are several evaluation procedures specifically adapted to rammed earth fortifications. Considering the analysis of materials, several authors have defined the

* Corresponding author. Av. Reina Mercedes 4A, 41012, Seville, Spain.
E-mail address: jjdelrio@us.es (J.J. Martín-del-Rio).

https://doi.org/10.1016/j.jobe.2021.103381
Received 27 July 2021; Received in revised form 13 September 2021; Accepted 24 September 2021
Available online 25 September 2021
2352-7102/© 2021 The Authors. Published by Elsevier Ltd. This is an open access article under the CC BY-NC-ND license (http://creativecommons.org/licenses/by-nc-nd/4.0/).

type of samples, the tests, as well as some results in reference case studies [13–15]. Damage has also been addressed in the case of historic walls, developing specific categories and evaluation criteria [16]. In the same way, risks and threats have been studied in fortified enclosures in southern Spain [16,17]. Additionally, in recent years, rammed earth has been studied from the point of view of the material durability [18,19] in order to preserve this kind of architectural heritage. Finally, in order to integrate all available information and improve heritage management, other authors have proposed the use of geographic information systems (GIS) adapted to the architectural scale of the particular case of fortifications in urban enclosures [20].

Regarding the characterization studies of rammed earthen materials, they are geographically centred in the Iberian Peninsula, North Africa, and some isolated cases in China. In the province of Erradichia (Morocco), several samples of soils used in traditional walls were analysed to determine, among other things, their physical and chemical properties, mainly by X-ray diffraction (XRD) and Scanning Electron Microscopy (SEM) [21]. Also in Morocco, researchers opted for non-destructive tests, like Ultrasonic Pulse Velovity, to evaluate the state of degradation of certain earthen walls [22], showing that these non-destructive techniques can be used to qualitatively assess walls, but the correlation with mechanical properties is not yet clear. Minor destructive tests such as flat jack, hole-drilling, and mini-pressuremeter have also been investigated [23], obtaining more congruent results for the measurement of compressive strength using the first two techniques previously mentioned. For the Great Wall of China (Ming Great Wall) in Qinghai Province [24] some basic physical properties of the soils (liquid limit, plasticity, soluble salts, Unconfined Compression Strength (UCS) were determined to establish a hierarchy of contributing factors in the process of rammed earth degradation. Furthermore, this study gives great importance to soluble salts in the degradation and stability processes of a rammed earth wall. In a geographical area closer to our study, the work on fortifications in the province of Granada (Spain) particularly stands out as one of the first studies on the physical-chemical characterisation of military rammed earth. Ontiveros-Ortega et al. proposed XRD to establish mineralogy, SEM and Hg-intrusion porosimetry to evaluate void distribution [25]. Likewise, among other issues, they conclude on the importance of water and the combination with soluble salts, such as sulphates, in the generation and evolution of lesions related to the loss of cohesion. Later, in the same field, the methodological proposal was improved with other analytical techniques such as X-ray fluorescence (XRF) and thermogravimetric analysis (TGA) with mass spectrometry (MS) to complete the chemical characterization of the walls with different restoration techniques by $Ca(OH)_2$ consolidation [26]. Following the guidelines of the work developed in Granada, another characterization of similar materials was carried out in the Castle of Mula (Murcia) [27], mainly with XRD microscopy and petrography, as a support to evaluate the state of preservation. However, it does not present or discuss the physical or mechanical properties of rammed earth, so the conclusions are supported by the tests mentioned above. In the Castle of Paderne (Portugal) [28] a material study of the walls, which have a similar chronology to that of the Walls of Sevilla, has been proposed by following similar guidelines to those specified by Alejandre et al. and Martín del Río et al. [13,14]. In this case, the study is focused on the chemical and mineralogical characterization, from which it is concluded that the aggregate is mostly calcareous and that lime was used as a binder. The study carried out to analyse the Urban Walls of Cáceres [29], also belonging to the same historical period, follows similar guidelines to those already described, and states that this rammed earth could be considered as a lime concrete since their great mechanical (up to 7 MPa) and the presence of lime (binder/aggregate ratio up to 2:5). In the eastern area of Spain, where this type of heritage is also frequent, it should be mentioned the study in the Castle of Villavieja (Castellón) [30] which, in the line of the previous ones, was focused on the definition of the lime-crusted walls.

Within a geographic scope closer to this study, several significant contributions can be found on very similar case studies. In the province of Sevilla, the materials of the Tower of D. Fadrique (Olivares) were characterized [31] showing high mechanical strength values and very low open porosity, making them similar to lime concretes. In Carmona, the materials of its Alcazar were analysed [32] and it also occurred with the Islamic Walls located in San Juan de Aznalfarache [33] or in the Castle of Luna from Mairena del Alcor [34], usually presenting lower quality materials in regard to their physical-mechanical properties. All of these cases follow the basic methodology already described by Martín del Río [14].

In relation to this kind of works, it can be said that, although this type of study has a moderate presence in the literature, there are not yet a large number of cases described in spite of the abundance of this type of heritage. Likewise, works on the relevant Sevilla Walls are particularly scarce. Only the study of Martín del Río et al. [35] which analysed two samples at Jardines del Valle and showed exceptional quality in terms of physical-mechanical properties. Recently, it has been developed an evaluation of the stability of walls under stress as retaining walls and applied to the case of Sevilla [36].

Legislation normally requires prior studies in case of heritage sites intervention, which usually include the characterization of materials. However, the types and scope of tests are highly variable and must be adapted to the particularities and needs of each case. In the particular case of military heritage built on earth, especially in the southern half of the Iberian Peninsula, it is necessary to establish contrasted procedures that serve not only as a support for the restorations, but also as a documentary corpus of scientific results that facilitate the knowledge of a construction system with highly variable material characteristics. However, these results are published on singular occasions, so there is a gap in the scientific literature dealing with rammed earth military walls. Additionally, many of these heritage assets are widely disseminated throughout the country and their locations sometimes are not easily accessible [37].

Therefore, the main goal of this research is to present and discuss the results of the materials' characterization of the Sevilla Walls, focused on the physical, chemical, and mechanical properties of the rammed earth. These results will serve to establish the main distinctive characteristics of this type of construction material, which is so common in medieval fortifications in the Iberian Peninsula. It is also intended that a cross-sectional reading of certain results will shed light on some of the keys to the pathological process currently observed in the structures analysed. The characteristics of the materials will serve as a basis for establishing intervention strategies for this monument and other similar ones that respect their heritage values, guarantee their material compatibility, and solve the pathological processes that most frequently affect this type of monumental structures.

This research is based on an experimental procedure for military rammed earth, the suitability of which has already been proven in other recent studies [13,14], offering valuable results for their restoration. The novelty presented in this study is twofold, since a procedure adapted to military rammed earth is applied to a monument that has never been studied in this depth, and the results are analysed and discussed in order to establish more suitable intervention criteria. Furthermore, in contrast to that reference procedure, a more detailed protocol has been developed to analyse and evaluate the transport of soluble salts.

2. Case study

Sevilla is located on the autochthonous fill of the Guadalquivir river basin whose chronostratigraphic formations range from the Tertiary to the Quaternary. The Macarena Wall, in particular, lies on a formation of silts, red and brown clays and medium to fine-grained sands, with cross stratification [38].

The Walls of Sevilla, whose origin is debated between the 12th and 13th centuries AD. [39], was one of the largest fortified urban enclosures in the Middle Ages in Spain. Covering approximately 273 ha and 6 linear

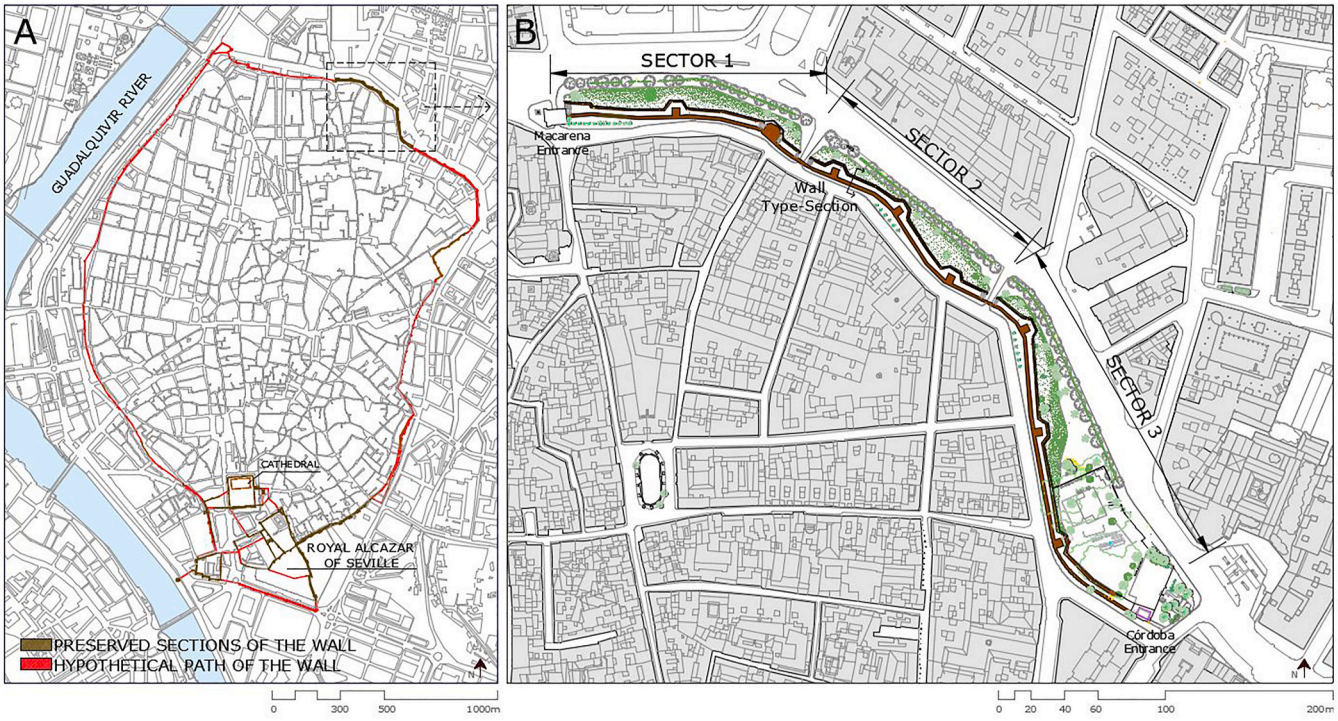

Fig. 1. *Plans of Sevilla: A) Sevilla city centre and the 14*th *century Walls B) One of the most relevant and preserved areas from the Wall: the Macarena Wall.*

Fig. 2. General views of area of the Wall under study.

km in the Almohad period, this military structure was maintained until the 19th century, when urban renewal processes triggered the demolition of many sectors. This Islamic fortification, as already mentioned, was built almost exclusively with rammed earth, with the exception of some decorative brick courses in the towers and upper parts of the walls.

Currently, the sector known as the Macarena Wall (Fig. 1a and b), located at the north of the ancient city, is the most relevant fragment of approximately 500 m in length, comprising walls, barbicans and towers. This military structure is formed by a main wall of 1.7–1.8 m thick and an average height of 8.0 m, a barbican of 1.3 m thick and 5.0 m high, a

Fig. 3. Damages observed in the visual inspection: A: Biodeterioration, B: Erosion, dirt, C: lack of cohesion, D: Dirt in lower areas, E: Loss of mass, F: Cracks.

ditch, and a moat. The Macarena Wall -divided into 3 different sectors or areas for better understanding-constitutes the case study of the present work (Figs. 1b and 2).

Conservation interventions of the Sevilla Walls, according to modern restoration canons, began in the 1980s and have continued until the first decade of the 21st century. Interventions carried out on the wall, most of them related to rammed earth, currently include a series of additions, replacements and restorations that show different levels of effectiveness. The first restorations were mainly carried out in the current sector of the Macarena Wall [40,41], although there were other relevant interventions in the sectors corresponding to the Jardines del Valle or La Moneda [42,43]. There have also been a great number of punctual interventions in emerging sectors of the wall within the historical city centre that showed uneven criteria and responses. The last significant intervention took place in 2008 and focused on the easternmost sector of the Macarena Wall [44]. From 2020 onwards, the last phase of interventions is being carried out in the sector of the Macarena Wall, which was partially supported by results presented in this study [45].

Precisely, considering the different overlapping of the construction stages and these restoration interventions, the study of materials is proposed to clarify the main degradation processes that currently affect rammed earth. The walls and towers of the Macarena Wall are suffering a progressive degradation process that mainly affects the materials' cohesion and leads to weathering and loss of mass (Fig. 3). The influence of water, either as an external weathering agent or as moisture content in the material, has been analysed for mechanical properties [46], durability [47] or within the cycles crystallization of salts [48] in rammed earth. The working hypothesis suggests that water plays an important role in weathering processes and mass loss, showing currently very evident symptoms on a significant part of the case study (Fig. 3).

3. Materials and methods

The military rammed earth is the material used for the fortification

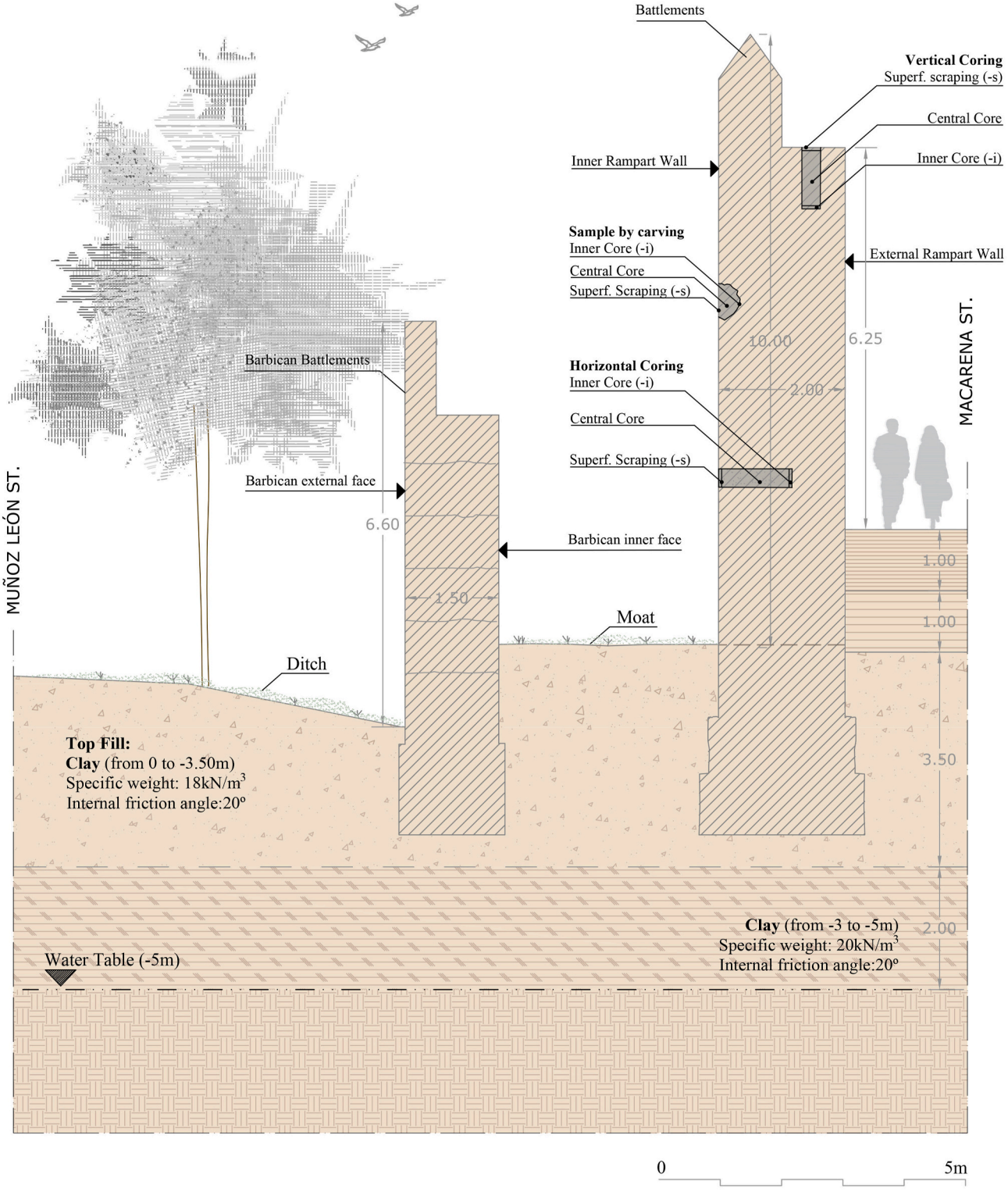

Fig. 4. Simplified cross section of the Wall and the barbican.

analysed in this research. According to several authors [6,7,35], this kind of material has similarities with the common rammed earth in terms of its construction technique principles, as both techniques use formworks where a material is compacted. However, the materials differ, since in the military version the lime content tends to be much higher, as well as a larger maximum aggregate grain size, which makes them more similar to lime concretes, with high mechanical performance, as indicate previously mentioned authors [35].

3.1. Extraction and designation of the samples

Three types of samples were taken, corresponding to carvings, scrapings and drillings (Fig. 4 and Fig. 5). The first ones were carried out mechanically, using a jack hammer trying to collect a sufficiently representative amount, between 5 and 10 kg. In these samples, the external face and the orientation of the compaction layers were identified in order to establish the logical direction for the unconfined

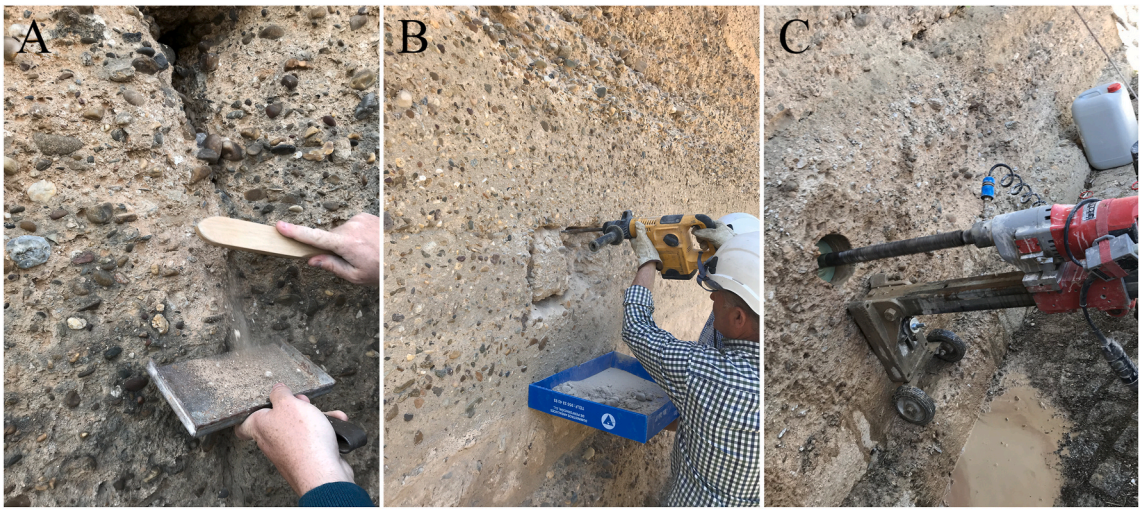

Fig. 5. Surface cleaning by brushing (A), mechanical milling (B) and sample extraction by drilling (C).

Table 1
Identification and location of core-samples and cylindrical specimen in the Macarena Wall.

compression test or to take additional samples, if necessary. These samples were used for chemical, mineralogical, physical and, in specific cases, mechanical determinations. In addition, all samples were weighed and bagged to establish moisture content.

Additionally, in some specific locations (Figs. 4 and 5c), several drillings were carried out with a cylindrical coring machine of 150 and 100 mm in diameter. They allow to extract material in depth, vertically and horizontally, and at various heights, mainly for mechanical, physical (bulk density and open porosity) and XRD tests.

Samples shown in Table 1 were designed by following the scheme in Fig. 6:

Apart from cylindrical specimen S3.4, all the samples were located in the lower courses of the wall, because the last two correspond to a different construction phase, which is not the object of the restoration intervention. The samples were taken on the external face of the Macarena Wall (Fig. 7), according to the three sectors defined in Fig. 1b. Samples of restored ("-R") and original ("-O") walls were also segregated, being all samples undisturbed except for the cylindrical specimens.

In summary, 18 locations were established in the main wall of the fortification and a total of 46 samples - cylindrical specimens and carved samples-were taken for the different physical (bulk density, open porosity, and grain size distribution), chemical, mineralogical, and mechanical (UCS) tests (Fig. 8).

3.2. *Chemical analysis by X-ray fluorescence (XRF) and carbonate contents*

For the quantitative chemical determination by XRF of the majority and minority elements (Si, Al, Fe, Mn, Mg, Ca, Na, K, Ti, P, S, F, Cl and S) corresponding to the total of the samples, it was used the Panalytical X-ray fluorescence equipment model AXIOS, which allows the chemical characterization (elemental range from Na to U) of samples of different sizes, in solid or powder form. The anti-cathode of the X-ray tube is Rh and the detector is an energy dispersive X-ray detector. The analysed portions come from the previously crushed and quartered mass.

The determination of the carbonate content (expressed as $CaCO_3$) was carried out by attack with 33% concentrated hydrochloric acid and calculating the difference in weight after the end of test. Carbonate determination is valid for approximating the original lime content (Ca $(OH))_2$ in walls made with it since over time the lime carbonates and becomes calcium carbonate. However, it must be recalled that both the earth and the aggregates used in its manufacture may naturally contain carbonate fractions. Therefore, the entire carbonate content is not always attributable to the addition of lime.

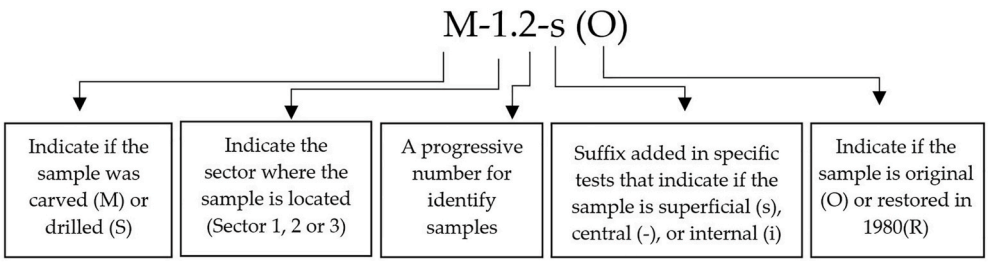

Fig. 6. Criteria followed to name samples.

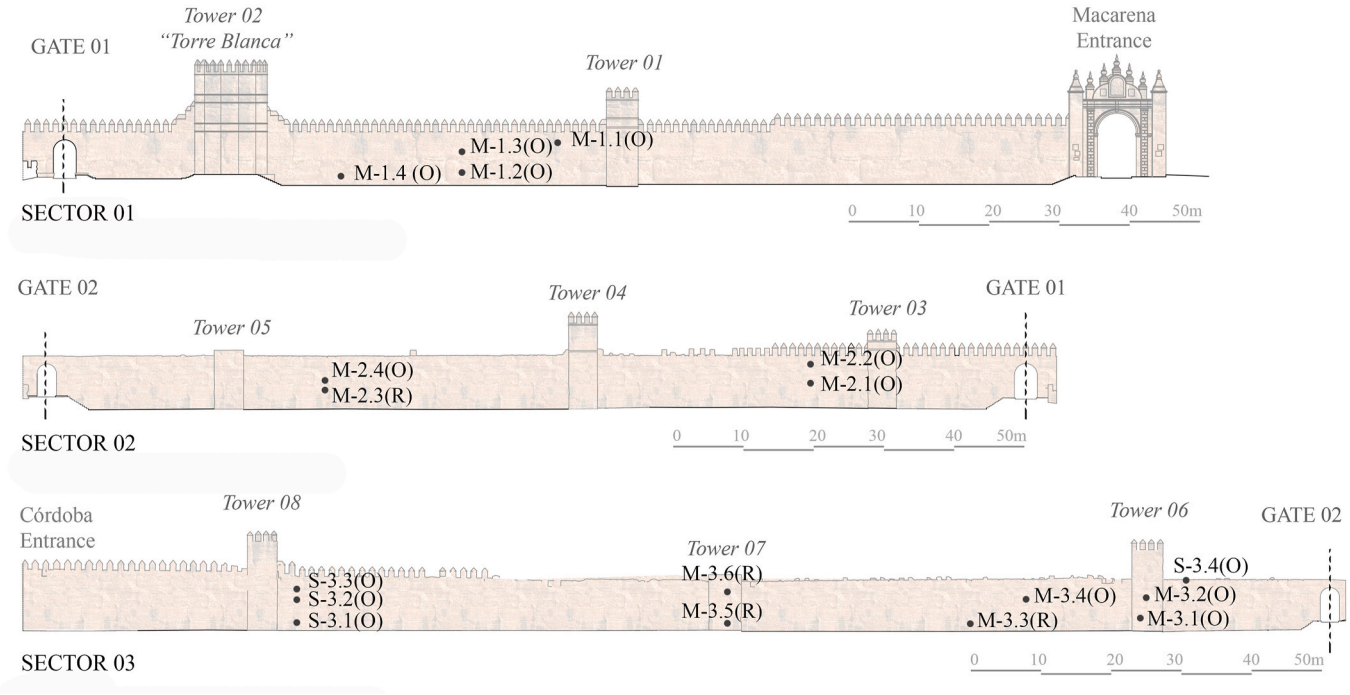

Fig. 7. Extramural elevations of the Macarena Wall. Location of sampling and boreholes.

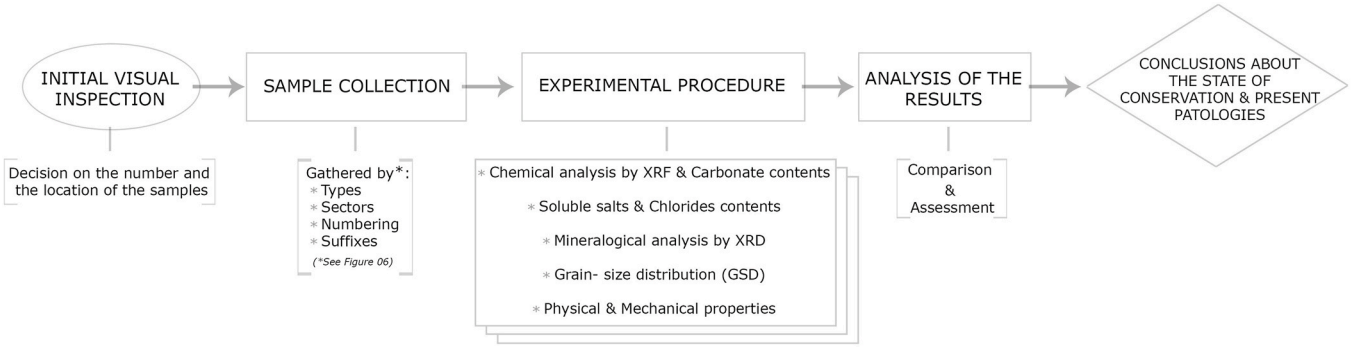

Fig. 8. Flowchart performed in this study.

3.3. Soluble salts and chlorides contents

In order to analyse the soluble salts in the 18 selected areas, a scraping with a metal bristle brush was carried out to collect between 50 and 100 g of material, prior to the described carving. This quantity corresponds to the surface sample and was designated with the suffix "-s" (Eq. (1)). By scraping, the intention is to extract only the fine material, avoiding the coarse fractions, which do not affect the salt analysis. After that, the inner side of the extracted sample was brushed again to take the same amount of material, corresponding to a depth of 15–12 cm, to check if there is any change in the concentration of salts in deeper layers. In this case, inner samples were noted with the suffix "-i" (Fig. 6).

In order to determine the content of soluble salts in the samples by inductively coupled plasma optical emission spectrometry ICP-OES, the extraction system indicated in UNE-EN 772-5 [49] has been applied. Once the samples were ready, they were taken to an atomic emission spectrometer by inductively coupled source, Horiba Jobin Yvon brand, ultima 2 model, hydride generation chamber Horiba Jobin Yvon brand,

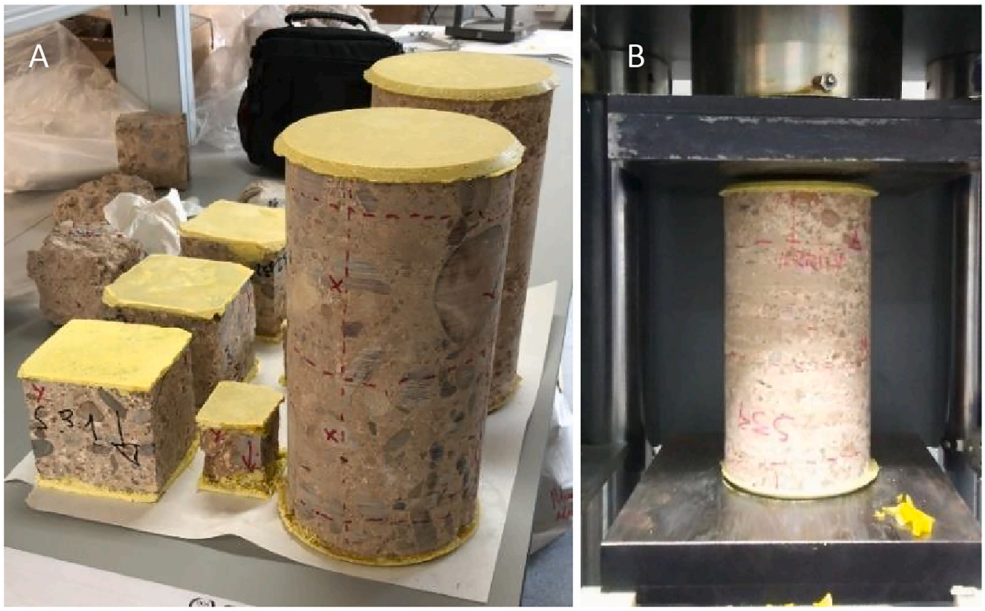

Fig. 9. Cubic and cylindrical wall test tubes faced with sulfur mortar (a). Test tube from borehole S-3.4 in the test press (b).

ultrasonic nebulizer CETAC AT + brand. Elements specified in standard UNE-EN 772-5 [49] were analysed: Na^{+}, K^{+}, Mg^{+2} and other unspecified ones such as Ca^{+2} and S.

The determination of chlorides in solution was carried out by ion chromatography with a Metrohm 930 Compact ICFlex Ion Chromatograph, using 20 g of sample in 250 ml of distilled water. As mentioned above, the material analysed corresponded to scrapings from the outer ("-s") and inner ("-i") surfaces of each sample.

3.4. Mineralogical analysis by X-ray diffraction (XRD)

In order to analyse mineralogy by X-ray diffraction in the 18 selected areas, the same process followed for soluble salts was followed. A scraping with a metal bristle brush was carried out to collect between 50 and 100 g of superficial material (-s) and the inner side of the extracted sample was brushed again to take the same amount of material, corresponding to a depth of 15–12 cm (-i), in order to check if there is any change in the concentration of salts in deeper layers.

The mineralogical analysis was carried out by X-ray diffraction (XRD) using a Bruker-AXS diffractometer model D8 Advance, identifying the overall mineralogy by the powder method. The results may be compared with XRF, carbonates or soluble salts determinations.

3.5. Grain-size distribution (GSD)

The grain-size analysis is performed after the attack with 33% concentrated hydrochloric acid to eliminate the carbonate lime matrix that acts as a binder of the particles and grains of the rammed earth. The required quantities were firstly crushed and quartered and then it was obtained a grain-size distribution that allows to separate the siliceous-silicate fraction when disaggregating each sample. To determine the grain size according to AENOR [50], it was used the disaggregated material from the washing and drying of the remains of the carbonate determination, differentiating the samples taken from the original rammed earth (O) and the ones from the restored parts (R). The fineness modulus was calculated through equation (1):

$$Fineness\ modulus = \frac{1300 - \Sigma\ percentage\ passing\ (\%)}{100} \quad (1)$$

3.6. Physical and mechanical properties

The physical properties determined are bulk density and porosity accessible to water (open porosity), all of which are characterized by providing information on the internal structure of the material (compactness). The method used for the determination of these properties is based on saturation of the sample with water under vacuum

Table 2
Chemical composition of majority and minority elements in the samples from XRF (weight %).

Sample	SiO_2	Al_2O_3	Fe_2O_3	MnO	MgO	CaO	Na_2O	K_2O	TiO_2	P_2O_5	SO_3	LOI	Total
M-1.1 (O)	**74.87**	4.44	2.09	0.04	0.62	7.78	0.59	1.01	0.26	0.09	0.64	8.11	100.52
M-1.2 (O)	**66.37**	6.09	2.34	0.05	0.71	10.66	1.38	1.31	0.32	0.11	0.69	11.60	101.63
M-1.3 (O)	44.13	6.30	2.57	0.05	0.93	**20.17**	1.26	1.85	0.37	0.15	0.25	**22.33**	100.37
M-1.4 (O)	**73.16**	4.29	1.89	0.04	0.60	9.02	0.91	1.12	0.26	0.09	N.D.	9.21	100.81
M-2.1 (O)	**72.13**	4.04	2.02	0.04	0.61	9.09	0.98	1.00	0.20	0.06	N.D	9.66	99.94
M-2.2 (O)	**64.93**	5.88	2.55	0.08	0.84	11.55	0.95	1.10	0.41	0.10	0.42	12.11	100.92
M-2.3 (R)	**69.46**	5.07	3.93	0.09	0.81	8.99	0.65	0.74	0.35	0.07	0.29	9.49	99.95
M-2.4 (O)	**78.09**	3.51	1.44	N.C.	0.34	7.43	0.70	0.81	0.20	0.05	N.D.	7.26	99.94
M-3.1 (O)	**61.55**	6.84	3.01	0.07	1.02	12.52	1.11	1.18	0.35	0.11	0.64	11.40	99.80
M-3.2 (O)	**70.82**	4.79	1.99	0.04	0.55	9.68	0.72	1.14	0.25	0.08	N.C.	9.97	100.26
M-3.3 (R)	**78.71**	4.28	2.26	N.C.	0.52	6.19	0.89	0.78	0.24	0.07	0.27	7.40	101.64
M-3.4 (O)	**63.26**	9.18	2.92	0.04	1.01	8.38	1.84	3.16	0.28	0.07	N.D.	9.89	100.20
M-3.5 (R)	**69.43**	3.79	2.09	N.C.	0.47	11.49	0.93	0.81	0.22	0.07	0.28	9.76	99.36
M-3.6 (R)	**71.60**	4.78	2.65	0.04	0.74	9.40	0.91	0.78	0.35	0.08	0.26	8.65	100.24

N.C.: Not quantified; N.D.: Not detected; LOI: Loss Of Ignition.

Table 3
Results of hydrochloric acid attack for estimation of carbonate content and maximun dossage in lime.

SAMPLE[a]**	%$CACO_3$ PER SAMPLE	%$CACO_3$ AVERAGE	REFERENCE LIME MORTARS (DOSAGE BY WEIGHT LIME: SAND) VS % $CACO_3$
M-1.1 (O)	15.48	15.32	1:1 57.5%
M-1.2 (O)	15.91		1:2 40.0%
M-1.4 (O)	17.58		1:3 31.0%
M-2.1 (O)	13.06		1:4 25,2%
M-2.2 (O)	13.01		1:5 21,3%
M-2.4 (O)	12.71		1:6 18,4%
M-3.1 (O)	16.93		1:7 16,2%
M-3.2 (O)	20.07		1:8 14,4%
M-3.4 (O)	13.14		1:9 13,1%
M-2.3 (R)	12.75	11.96	1:10 11,9%
M 3.3 (R)	11.62		
M-3.5 (R)	12.26		
M-3.6 (R)	11.22		

**Class: Sample from original rammed earth (O), sample from repaired rammed earth in the 1980s (R).

[a] It has not been possible to take sufficient sample for the analysis of M-1.3.

according to the standards [51]. For this test, pairs of samples, named "a" and "b", were taken from the main carved sample.

For the determination of the UCS nine specimens were tested, the position and orientation of the carved or cored samples have been taken into account. Three cylindrical cored samples 15 cmØx30 cm, namely S-3.1c, S-3.1d and S-3.4, were tested in the direction perpendicular to the compaction since they were extracted horizontally, for these same cylindrical specimens it has been possible to cut out cubic specimens with 10 cm side (S-3.1a, S-3.1b), which were tested in the compaction direction (Fig. 9), and finally four carved cubic specimens (M-1.1, M-1.3a, M-1.3b and S-3.2) with 6 cm side. Based on the differences in slenderness of the samples, which range from 2 for cylindrical samples to 1 for cubic samples, and according to the correction coefficients [52,53], the values of the cubic samples of slenderness 1 have been corrected by the coefficient 0.9. These specimens have been capped with sulfur mortar and tested in a TCCSL press, model PCI-30 Tn, with a loading rate of 323 N/s, according to the standard [54,55], the specimens were dried to have constant moisture content.

4. Results and discussion

The results of the samples and specimens analysed, as well as a discussion of the results, are presented below.

4.1. Chemical analysis by XRF and carbonates contents

The high SiO_2 content (Table 2) may be expected due to the component of a rammed earth, highlighting the aggregate of a siliceous-silicate nature, mainly quartz and feldspars, phyllosilicates and inosilicates as minorities (see section 4.3.). The percentage of CaO has been low, except in the case of sample M-1.3, being mainly attributable to the presence of $CaCO_3$. If these results are compared with those of the study carried out by González Díez [56], in which they have stated that the geological origins of the city of Sevilla range from the Miocene-Pliocene to the alluvial Quaternary, these samples are quite similar to those of the Quaternary level, where quartz is the main mineral.

The SO_3 content has oscillated between 0.25% and 0.69%, and if it were expressed as gypsum ($CaSO_4{\cdot}2H_2O$), the interval would be between 0,53% and 1,48%, indicating gypsum was not used as a binder in either wall.

The carbonate contents expressed as $CaCO_3$, was established by hydrochloric acid attack. Likewise, it is possible to recognize how the highest carbonate contents are mainly associated with the original rammed earth, in the range of 10–20%, with an average of 15.32%. In comparison, the samples from the restoration of the 1980s (M-2.3, 3.3, 3.5 and 3.6) correspond to medium or low values, with a range between 11 and 13%, with an average of 11,96% (Table 3). If these values are compared with reference lime mortars (Table 3), it could be set a maximum dosage in lime between 1: 6 and 1:10 for the original rammed earth walls, and from 1: 9 to 1:10 for the restored ones. However, it must be considered that the aggregate used in its preparation may naturally contain carbonate fractions, which is the reason why not all of the carbonate content is always attributable to the addition of lime. In this case, it could only be dealing with maximum lime addition contents and not with real contents.

As these are compacted earthworks, these dosages should not be considered low, being recommended by literature contents of lime around 4–5% [57]. Therefore, with this criterion, analysed samples can be considered rich in lime, as is usual in samples of military rammed earth, even considering the deviations of the acid attack.

In sample S-3.1a -a horizontal core-the inner section, located at 95 cm deep, is not yet carbonated (Fig. 10 B). That could be verified thanks to the phenolphthalein turnaround in contact with the basic pH of calcium hydroxide. In Fig. 10 it can be seen how the first 25 cm approximately show carbonation as there is no colour change in the deposited phenolphthalein. From these 25 cm onwards, the carbonation front is clearly visible first, followed by the non-carbonated sections (Fig. 10 A) up to the maximum depth reached by the sample at 95 cm (Fig. 10 B). Despite this circumstance, the mechanical strength of the internal sections of the wall has not been greatly reduced for this sample in relation to other samples (see section 4.5). In contrast to lime-crusted rammed earth, where the lime is concentrated in the outer layer [30], in this type of rammed earth, lime is present throughout the thickness of the wall and in a considerable proportion of the wall. For these reasons, these types of rammed earth walls have been referred to as lime concretes by some authors [3,58].

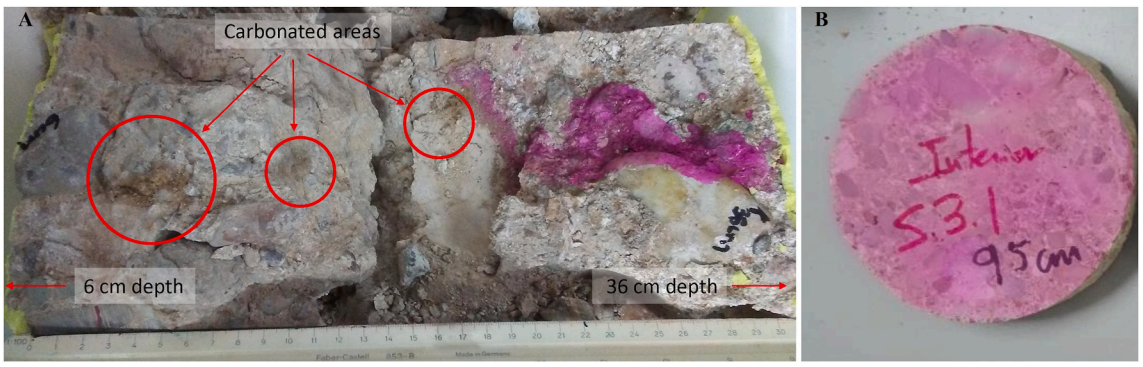

Fig. 10. Phenolphthalein test at different depths (cm) of drilled samples. A: inner core of the sample S-3.1 after the UCS test. B: Cross-section of sample S-3.1 at the innermost part.

Table 4
Chemical composition of soluble salts extracted from rammed earth samples from distilled water leaching and chloride content (mg/l).

SAMPLES	CLASS CONDITION HEIGHT (M)			mc (%)	CA^{+2} (MG/L)	K^{+} (MG/L)	NA^{+} (MG/L)	MG^{+2} (MG/L)	S (MG/L)	CL^{-}(MG/L)
M-1.1-S	O	++	6.0	2.3	1549.0	70.6	208.0	25.0	734.0	321.38
M-1.1-I					1112.0	51.6	255.0	27.2	271.0	423.00
M-1.2-S	O	++	1.4	1.8	1206.0	159.0	278.0	31.3	908.0	393.77
M-1.2-I					239.0	107.0	195.0	15.5	118.0	267.00
M-1.3-S	O	+++	3.7	1.7	1601.0	270.0	468.0	24.6	229.0	959.14
M-1.3-I					1385.0	308.0	437.0	20.6	399.0	788.00
M-1.4-S	O	++	0.9	8.3	1322.0	361.0	440.0	35.1	830.0	508.32
M-1.4-I					350.0	493.0	821.0	26.3	117.0	1003.00
M-2.1-S	O	+++	4.0	3.2	765.0	109.0	416.0	19.2	22.5	667.32
M-2.1-I					986.0	171.0	574.0	42.0	138.0	836.00
M-2.2-S	O	++	6.0	4.0	958.0	70.1	124.0	17.7	362.0	356.76
M-2.2-I					/	/	/	/	/	/
M-2.3-S	R	+++	3.0	5.0	842.0	99.5	289.0	6.5	251.0	336.92
M-2.3-I					136.0	36.5	111.0	3.4	415.0	104.00
M-2.4-S	O	+++	4.0	4.1	838.0	80.2	369.0	12.7	33.6	527.27
M-2.4-I					863.0	68.3	441.0	13.8	279.0	566.00
M-3.1-S	O	++	1.6	1.6	859.0	103.0	131.0	25.4	613.0	134.93
M-3.1-I					715.0	105.0	151.0	18.5	268.0	157.00
M-3.2-S	O	+	4.8	3.5	359.0	20.8	12.3	3.7	316.0	40.77
M-3.2-I					732.0	112.0	158	13.2	859.0	410.00
M-3.3-S	R	+	1.6	1.8	1102.0	19.9	27.0	2.6	989.0	23.20
M-3.3-I					111.0	8.4	22.5	1.8	258.0	35.60
M-3.4-S	O	++	4.8	2.0	690.0	54.4	142.0	10.3	113.0	328.00
M-3.4-I					1210.0	44.3	280.0	15.2	719.0	624.00
M-3.5-S	R	++	1.8	5.3	520.0	60.2	141.0	2.8	159.0	259.00
M-3.5-I					376.0	54.4	133.0	2.9	762.0	230.00
M-3.6-S	R	+	4.7	/	749.0	33.9	79.0	3.2	626.0	121.46
M-3.6-I					/	/	/	/	/	/
S-3.1-S	O	+	0.8	/	1312.0	596.0	860.0	53.4	679.0	626.63
S-3.1-I					53.3	15.1	38.4	0.1	3.2	/
S-3.2-S	O	++	4.3	/	412	78.0	89.5	7.4	359.0	117.96
S-3.2-I					/	/	/	/	/	/
S-3.3-S	O	++	6.0	/	53.1	15.3	56.0	0.2	4.1	11.60
S-3.3-I					669.0	42.9	14.1	4.6	643.0	/
S-3.4-S	O	+	7.0	/	/	/	/	/	/	/
S-3.4-I					38.5	14.7	14.4	0.1	2.9	/

Condition: (+) cohesive, slightly deteriorated, (++) lack of cohesion, deteriorated, (+++) sandblasted, very deteriorated, (/) it has not been possible to extract a sample. O: original rammed earth; R: restored rammed earth; MC: Moisture Content.

4.2. Content of soluble salts and chlorides

The contents of soluble salts are shown in Table 4 of the samples extracted and analysed following the procedure described in the methodology. For this purpose, the contents of the superficial part ("-s") are compared with the corresponding contents of the internal one ("-i").

Comparing the ranges of concentrations obtained, Ca^{+2} stands out as the one that reaches the highest proportions (38–1601 mg/l); on the contrary, Mg^{+2} is the one with the lowest range (0–53 mg/l). Soluble sulphates, evaluated by sulfur (S), have an outstanding presence which, although they are not the highest, their maximums are more distributed among the entire collection of carved and cored samples, while the maximum values of Ca^{+2}, K^{+}, Na^{+} and Mg^{+2} are concentrated in sector 1 and part of sector 2.

Firstly, Cl^{-}, K^{+} and Na^{+} ions that form highly soluble salts (mainly chlorides and nitrates) have a higher concentration at a height of 3–4 m (Fig. 11). This distribution and fractionation of ions along the capillary ascent zone has already been described by other authors [59]. However, this relationship, which would support the hypothesis of a mechanism of salt transport by capillarity, is not fulfilled in the case of samples M-1.2, M-2.3, M-3.1, M-3.3, M-3.5. In these cases, the concentrations of salts (Cl^{-}, K^{+}, Na^{+}) in the inner wall are lower and do not correlate with the height which, on the contrary, is found for the rest of the samples in the same soluble salts (Fig. 11). This is evidence of a non-uniform distribution in the transport of soluble salts in the wall, which is also confirmed by the irregularity of the moisture contents recorded at different heights. As shown in Table 4, the moisture contents vary from 1.7% to 8.3% and without any correlation with the height of the samples themselves. It can be stated that the moisture contents corresponding to the aforementioned samples are not the highest, and correspond to low salt contents (Cl^{-}, K^{+}, Na^{+}). On the other hand, the highest moisture content corresponds to sample M-1.4 (8.3%), which also has the highest content of soluble salts (Cl^{-}, K^{+}, Na^{+}). Therefore, these facts show the relationship between soluble salts and moisture content, although according to an uneven distribution in the wall.

The fact of the uneven height distribution of moisture in the wall can be corroborated from thermographic camera readings (Fig. 12). Thermography, as a non-destructive technique, can be used to qualitatively map the moisture distribution in a porous wall due to capillary action [60]. As shown in Fig. 12, the lower part of the wall presents a 4-5 °C lower temperature, which reaches up to the third course of wall (2.7 m) on the outer face towards Macarena street, which on the inner face translates into a height of 5 m, coinciding with the ranges of the heights of the samples extracted on this face. In addition, it is also observed that the distribution of the coldest areas at the base is irregular, which may indicate that samples at similar heights have different moisture levels. Finally, we also note how the first course of wall shows a higher temperature, discordant with its surroundings (Fig. 12 a), which coincides exactly with the new material reinstated as a result of the 20th century restoration. This new material, although similar to the original, may present a higher porosity (up to 33.9%) and a lower compactness, as discussed in sections 3.5 and 3.6, which evidently influences a different behaviour with respect to the capillary water transport capacity and salt crystallization. It is precisely the original wall in contact with the

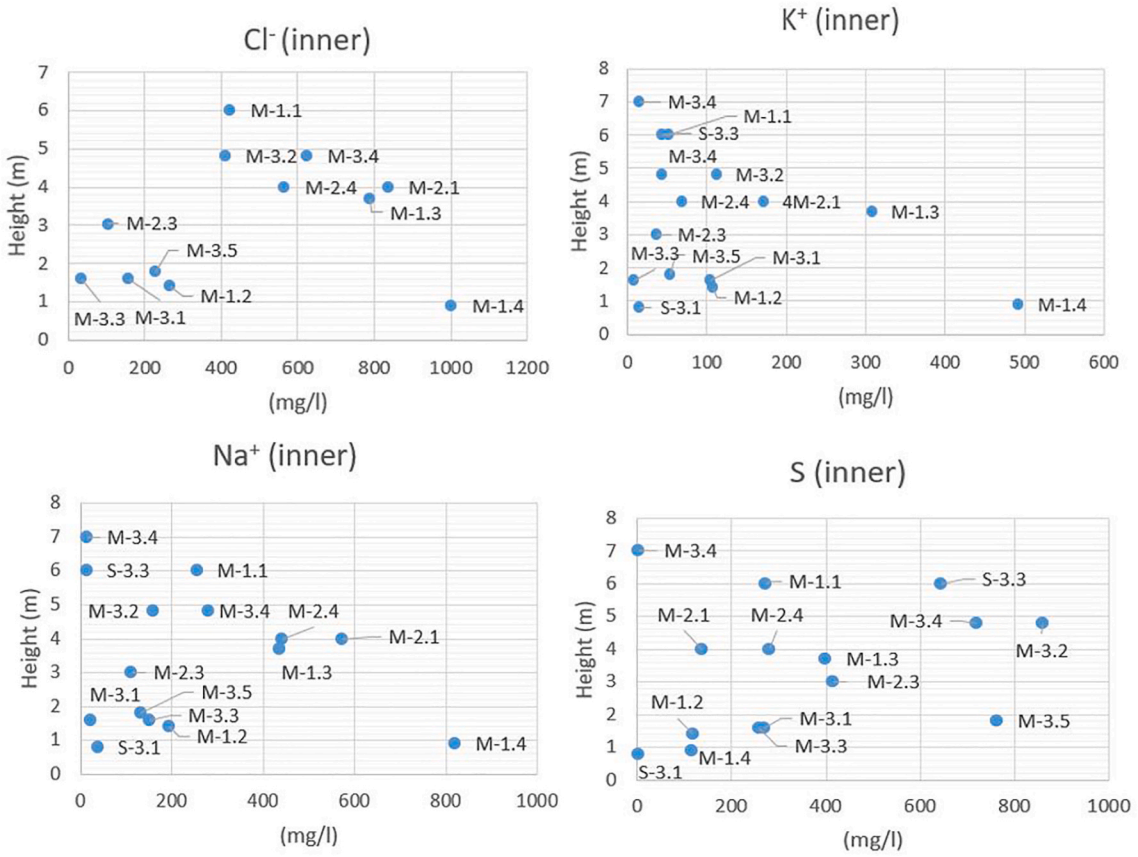

Fig. 11. Relationship of salt content to sample height (inner zone).

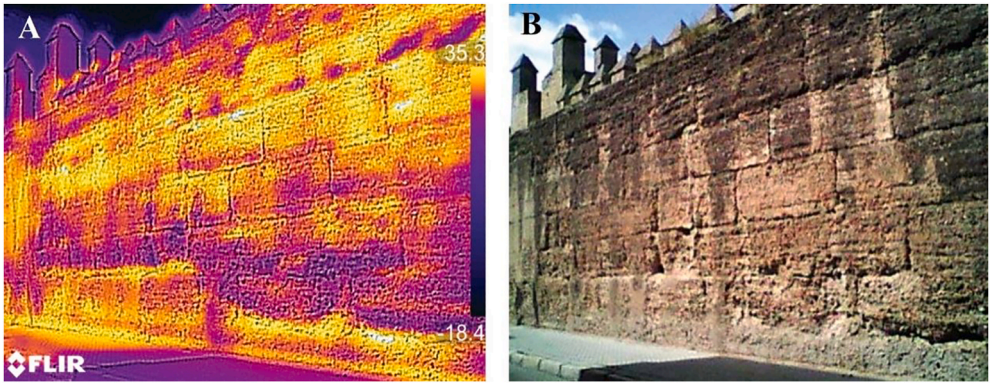

Fig. 12. Thermographic image (A) and real image (B) of the external face of the Wall generated by a Flir T420bx model camera (images taken in 4/9/2019 at 4:33 p.m.).

restored area that shows the highest mass losses (Fig. 12 b). Therefore, based on the evidence shown, it is possible to affirm that there is a differential behaviour of the wall depending on its salt content, its moisture content and its location, which leads us to think that capillary rising damp and the crystallization of salts are phenomena that are present and directly related to its state of conservation.

The results also show that salts migrate when dissolved in water, from the inside to the surface, where they crystallize [48]. This process usually leads to a higher concentration on the surface, where the increase in volume by crystallization internally stresses the pores of the material, causing its fracture. This loss of cohesion leads to weathering, disintegration and sandblasting of the outer layers (Figs. 3–4), so all loose material is removed, along with crystallized salts, from the surface. This may be the reason why there is an inverted relationship of salt concentrations between the inner and outer sides of the samples. The symptomatology detected in situ has been similar to that recorded in other rammed earth walls attacked by salts [61,62], which generates a crust that peels off and leads to a weakened interior due to the new crystallization of salts.

In general terms and comparing with similar cases like the one exposed by Shao et al. [62], the range of the percentage of chlorides is high. The soluble chloride content in the samples ranges from low values of 11.60 mg/l (S-3.3-s) and 40.77 mg/l (M-3.2-s) to higher values over 500 mg/l (samples M-1.3-s, M-1.4-s, M-2.1-s, M-2.4-s and S-3.1-s) for surface samples from more disturbed areas. In this sense, the areas associated with samples M-1.3, M-1.4, M-2.1 and M-2.4 show greater weathering and loss of surface mass.

The origin of the salts is diverse [63]. From external sources, from

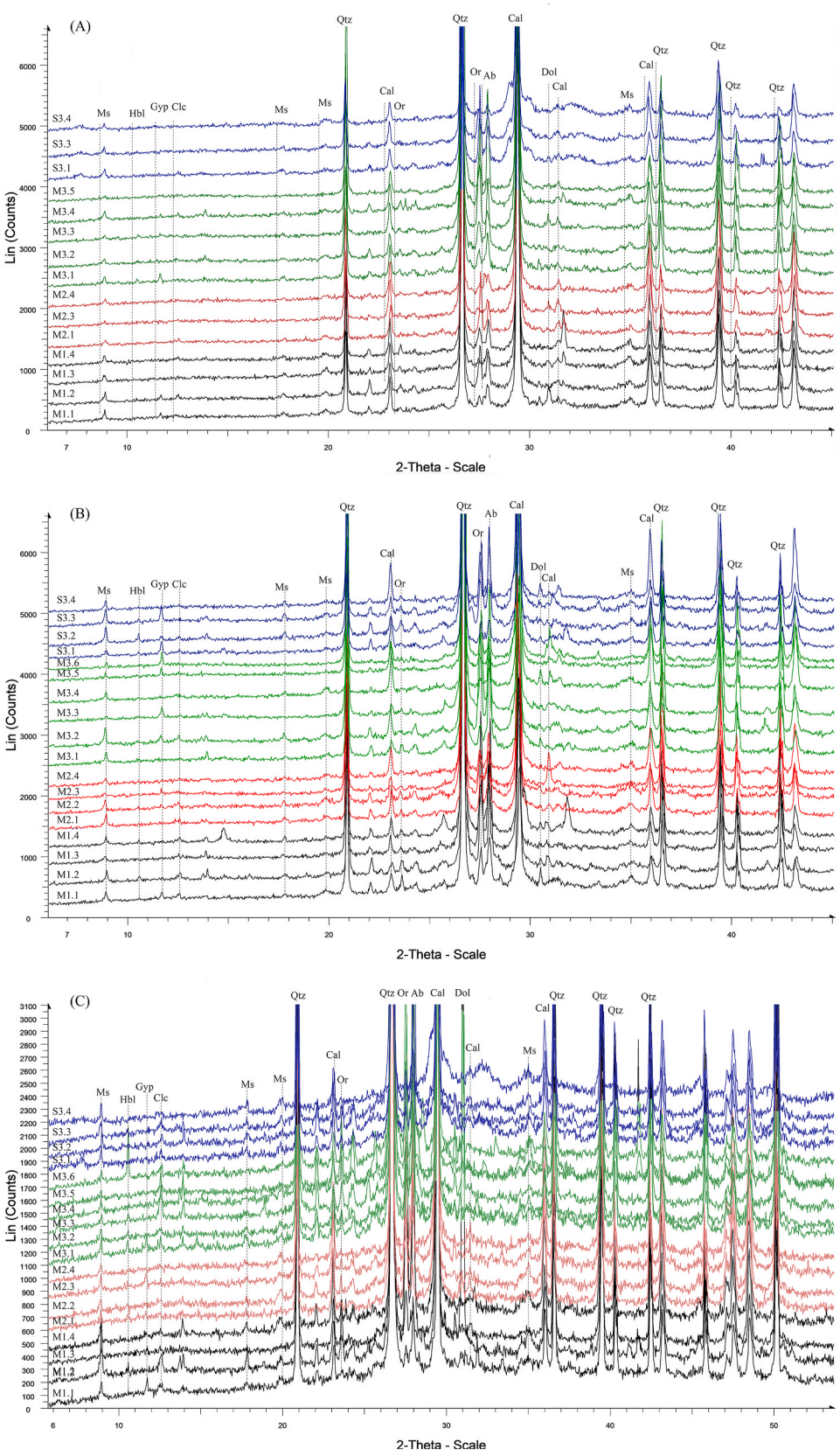

Fig. 13. Diffractogram of all samples according to their source: (A) inner, (B) superficial and (C) in their central section. In ascending direction: from bottom to top, sector 1 (black), sector 2 (red), sector 3 (green) and the cored samples (blue). [Gyp-Gypsum, Or-Orthoclase, Ab-Albite, Ms-Muscovite, Dol-Dolomite, Hbl- Hornblende, Clc-Clinochlore]. (For interpretation of the references to colour in this figure legend, the reader is referred to the Web version of this article.)

Table 5
Qualitative mineralogical composition of the samples and boreholes in its central part.

SAMPLE	Qtz	Cal	Gyp	Or	Ab	Ms	Dol	OTHER MINERALS (Tr)
M-1.1 (O)	++++	++	+	+	+	Tr	Tr	Hbl, Clc
M-1.2 (O)	++++	++	+	+	+	Tr	Tr	Hbl, Clc
M-1.3 (O)	++++	++	+	+	+	Tr	Tr	Hbl, Clc
M-1.4 (O)	++++	++	+	+	+	Tr	Tr	Hbl, Clc
M-2.1 (O)	++++	++	+	+	+	Tr	Tr	–
M-2.2 (O)	++++	++	+	+	+	Tr	Tr	–
M-2.3 (R)	++++	++	+	+	+	Tr	Tr	–
M-2.4 (O)	++++	++	+	+	+	Tr	Tr	–
M-3.1 (O)	++++	++	+	+	+	Tr	Tr	Hbl, Clc
M-3.2 (O)	++++	++	+	+	+	Tr	Tr	Hbl, Clc
M-3.3 (R)	++++	++	+	+	+	Tr	Tr	Hbl, Clc
M-3.4 (O)	++++	++	+	+	+	Tr	Tr	Clc
M-3.5 (R)	++++	++	+	+	+	Tr	Tr	Clc
M-3.6 (R)	++++	++	+	+	+	Tr	Tr	Hbl, Clc
S-3.1 (O)	++++	++	+	+	+	Tr	Tr	Clc
S-3.2 (O)	++++	++	+	+	+	Tr	Tr	Clc
S-3.3 (O)	++++	++	+	+	+	Tr	Tr	Clc
S-3.4 (O)	++++	++	+	+	+	Tr	Tr	Clc

Notation used: ++++ high proportion (>50%), +++ medium proportion (30–50%), ++ low proportion (10–30%), + very low proportion (3–10%), Tr. Traces (<3%), (−) not detected. Qtz: Quartz, Cal: Calcite, Gyp: Gypsum, Or: Orthoclase, Ab: Albite, Ms: Muscovite, Dol: Dolomite, Hbl: Hornblende, Clc: Clinochlore.

the soil, or from the environment due to contamination, or internal sources, such as constituent materials. In the case of the wall materials, the origin is not clear and could be attributed to several factors. In theory, the high presence of S in many samples from original rammed earth, and even in their internal parts (Table 4 and Fig. 11), may suggest that the main source is not atmospheric contamination. Rather, the origin may lie in the raw wall components themselves, in the presence of gypsum determined by XRD (section 4.3). Regarding chlorides, an environmental origin (from marine aerosols) can be ruled out. They would probably also come from the same raw material of the wall or capillary ascension, since, as can be seen, the presence of chlorides is higher in some inner samples (M-1.4, M-2.1, M-3.2, M-3.4, among others). In general and according to the degradation profiles observed in the surfaces (Fig. 10) and those described in the literature [64] we can confirm that capillary rising water is the main source of moisture that drives the transport of salts.

4.3. Mineralogy by XRD

The XRD mineralogical analysis of the carved and cored samples from the three sectors has been grouped according to their source: superficial and inner scrapping and central section (Fig. 13). Minerals detected on the surface and in the inner part are consistent with those established according to XRF.

Table 5 shows the majority minerals in the carved and cored samples, as well as other secondary minerals for the samples from the core part of the samples. Quartz stands out as the most abundant mineral, unlike other rammed earth that have a low calcite content, since their aggregates are mostly of siliceous and silicate origin [14]. Calcareous minerals can be found in smaller proportions, such as calcite, or in traces, such as dolomite. These results confirm the XRF data for the relationship between the siliceous-silicate and calcareous fractions. The presence of gypsum, which, although is not abundant comparing with other mineralogical components, can be enough to produce possible alterations by solubilization-crystallization cycles. In this sense, most of the samples (superficial, internal, or central) present gypsum, in accordance with the values established for sulphates based on soluble salts. Feldspars (orthoclase, albite) and phyllosilicates (muscovite/illite) are present in smaller proportions. All these minerals have their origin in the soil and lime used for the construction of the rammed−earth.

4.4. Grain size distribution

The grain size distribution curves of all the samples were plotted differentiating between the samples obtained from the original wall and from the restored wall areas. The ideal Fuller curve for granulometries with a maximum diameter of 60 mm was added as well as the area considered optimal for rammed earth walls according to Ref. [2], which is outlined by two curves, the upper and lower limits. It is necessary to clarify that, if the aggregate has a carbonated fraction and it is eliminated by the acid attack, the results obtained may have some alterations. However, given the high proportion of siliceous aggregate (64–78% according to XRF) over calcareous, these deviations have a minor impact, except in sample M-1.3. Except for this case, it is considered that the curves shown here are approximate to reality.

In the samples from the original areas of the Walls (Fig. 14A), the heterogeneity of the aggregate grain sizes used can be highlighted depending on the sector considered. The samples of Sector 2 are clearly different from those of Sector 1, since they show a continuous grain size that is generally closer to the ideal Fuller curve [2]. Curves from Sector 2 (Fig. 14B) are within the limits of the optimal zone [2] and their fineness modulus are within the acceptable range that delimit the fineness modulus of the upper and lower Fuller limits (Table 6), although with a higher proportion of the coarse fraction (>4 mm), around 70–80% of gravels.

On the contrary, the granulometric curves from Sector 1 (Fig. 14A) show a higher percentage of fine fractions (<4 mm) and a lower percentage of gravels (45–65%), where the sand fraction of all of them is above Fuller's upper limit, pointing out that they are finer than desirable. In this sector, only sample M-1.1 has the grain size distribution closest to Fuller's ideal, ratified by its fineness modulus.

In relation to the granulometries of sector 3 (Fig. 14C), they also present a higher proportion of fine fractions (particle size smaller than 4 mm) and a great variability in gravel that oscillates between 30 and 70%, being observed in the chart that the samples M.3.1 and M.3.2 at all times run above the upper Fuller limit, implying that both -the gravel and sand fractions-are finer than desirable, as confirmed by the fact that their fineness modulus are less than the modulus of the upper limit of Fuller. However, sample M.3.4 runs above the upper limit in the sand fraction and below the lower limit in the gravel fraction, suggesting that the coarse fraction is coarser than desirable, as confirmed by its fineness modulus that is greater than the modulus of the lower Fuller limit.

With regard to the fine content (percentage of aggregate which passes the sieve 0.063 mm), the ideal suggested by Schroeder [2] is small (<5%), compared to those calculated for these samples (4–17%). However, other authors suggest clay contents valid for rammed earth between 5 and 18% [65], therefore the values determined here can be considered correct for this type of construction.

Concerning the restored areas (Fig. 14D), it is noted that the fractions corresponding to coarse grain sizes are higher (60–70%), detecting unbalances between fine and coarse fractions. This is more evident in M.2.3, which presents a worse compaction due to a lack of fractions between 5 and 30 mm, confirmed by the high open porosity and low bulk density determined in Table 7. It can be seen that the materials used

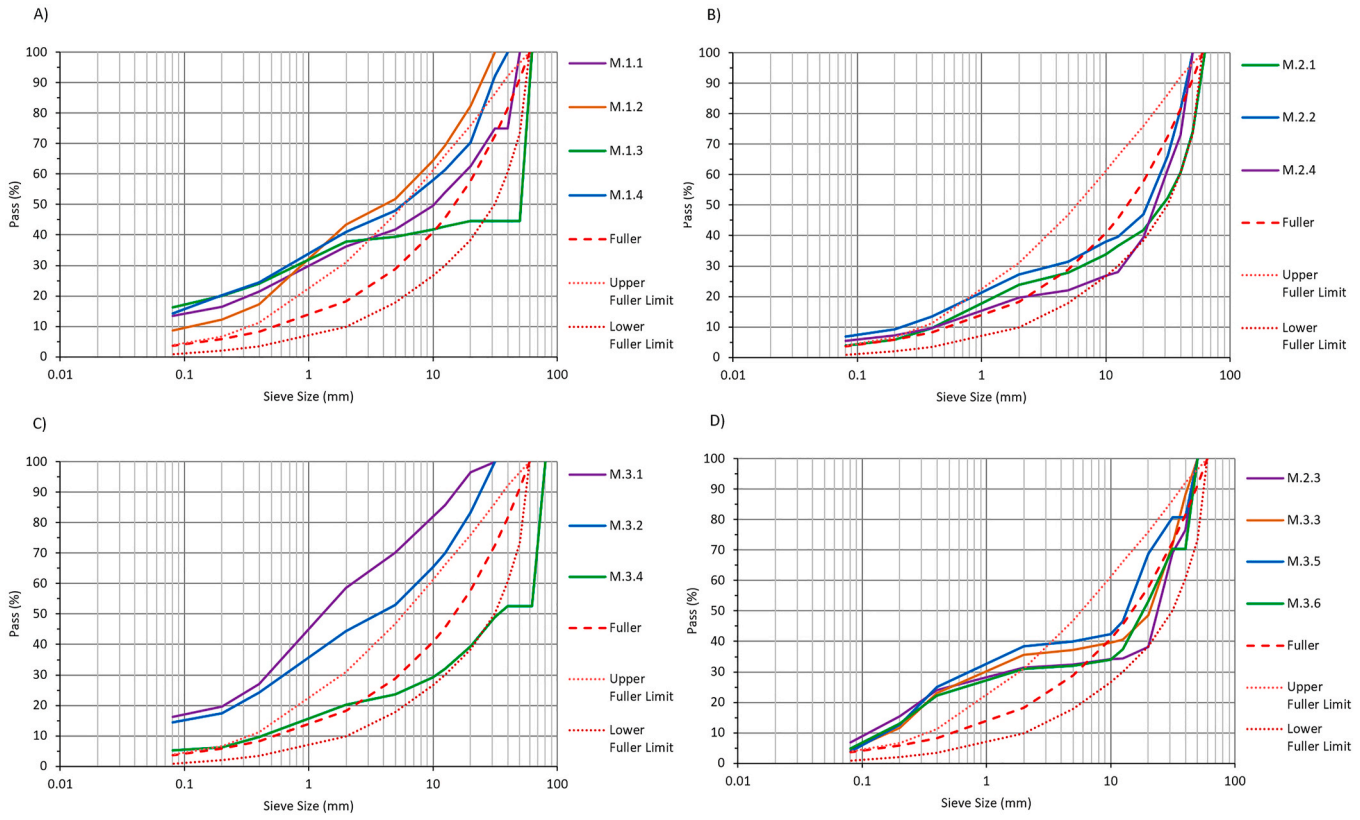

Fig. 14. Particle-size curves of samples compared with the ideal Fuller curve and the limit curves for aggregates with a max diameter = 60 mm. A) original areas of Sector 1, B) original areas of Sector 2, C) original areas of Sector 3 and D) restored areas of the wall.

Table 6
Fineness modulus of the studied samples and Fuller's and lower and upper limits.

Original Areas (O)										Restored Areas (R)				Fuller (60 mm)		
Sector 1				Sector 2			Sector 3									
M-1.1	M-1.2	M-1.3	M-1.4	M-2.1	M-2.2	M-2.4	M-3.1	M-3.2	M-3.4	M-2.3	M-3.3	M-3.5	M-3.6	Upper limit	Fuller	Lower limit
5.55	4.51	6.99	4.70	7.30	6.40	7.07	3.44	4.28	8.28	6.37	5.99	5.61	6.31	5.22	6.46	7.87

in the first stages of the restoration (sector 2) obeyed a non-optimal design criterion that was later corrected (sector 3). The sand fraction of all of them (M.2.3, M.3.3, M.3.5, M.3.6) is above Fuller's upper limit, suggesting that they are finer than desirable. However, fineness modulus of the samples from the restored areas are within the acceptable range outlined by the upper and lower Fuller limits (Table 6).

4.5. Physical and mechanical properties

The bulk density and open porosity values are shown in Table 7. Bulk density presents an average of 2 g/cm^3 with a coefficient of variation (CV) of 5.13% and open porosity with an average of 22%, CV of 20.5% and with a range of values between 14 and 30%.

Referring to other historical rammed earth or lime concretes walls, authors such as J.J- Martín-del-Río [35] establish porosities between 30% and 50%, which places these samples in a lower range. Bulk density of a rammed earth does not usually exceed 2–2.1 g/cm^3 [52]. Therefore, these rammed earth walls can be considered to have medium-to-high density. On the other hand, it can also be observed how the restored rammed earth samples (M-2.3, M-3.3 and M-3.5) present higher porosities. Open porosity also decreases from sector 2 (M-2.3 = 33.09%) to sector 3 (M-3.3 = 23.14%, M-3.5 = 20.85%). Therefore, being the restorations of sector 3 the most recent ones, it can be noticed that the quality of the materials has been improving, a fact that is also confirmed by the grain size analysis, which shows a better compaction.

When dealing with the mechanical performance, the three smaller cubic specimens (M-1.1, M-1.3a and M-1.3b) have lower strengths (Table 7), while their lower porosities are usually associated with higher mechanical strengths [66]. The results are likely to be affected by the high maximum aggregate size (40–50 mm) with respect to the specimen size. Additionally, as they are more superficial samples, they may be more altered by weathering, water seepage or salt crystallization. Also noteworthy is the lower strength of specimen S-3.4, which belongs to the two upper courses of the main wall, which are considered by some authors as a later construction phase and therefore with different construction characteristics [39].

Except for the cylindrical specimens (S-3.1a, S-3.1d), all were tested in the compaction direction. Comparing the resistances according to the test directions, it can be observed that the values are similar, which supports the hypothesis that this material could be considered as quasi-isotropic [67].

The depth of the sample in relationship to the thickness of the wall appears to be a factor affecting the compressive strength. In cored samples S-3.1, sample S-3.1a refers to the shallowest part with the highest resistance (8.26 N/mm^2), while S-3.1d is the deepest and least resistant (6.22 N/mm^2). As explained (see section 4.1), in samples at

Table 7
Physical-mechanical properties.

Samples	Type[a]	Bulk Density (g/cm^3)	Open Porosity (%)	Shape/size (LxWxH) cm (DxH) cm	Slenderness	UCS (N/mm2)	UCS corrected (N/mm^2)
M-1.1a	O	1.98	21.71	Cubic/6 × 6 × 6	1	5.01	4.51
M-1.1b		2.02	20.37				
M-1.2a	O	2.02	23.73				
M-1.2b		2.01	24.36				
M-1.3a	O	1.82	20.97	Cubic/6 × 6 × 6	1	3.49	3.14
M-1.3b		1.84	20.27	Cubic/6 × 6 × 6	1	4.53	4.08
M-1.4a	O	1.91	28.06				
M-1.4b		1.86	29.72				
M-2.1a	O	2.15	14.76				
M-2.1b		2.10	15.07				
M-2.2a	O	2.07	18.49				
M-2.2b		2.16	17.56				
M-2.3a	R	1.76	33.90				
M-2.3b		1.81	32.29				
M-2.4a	O	1.99	21.15				
M-2.4b		1.85	25.00				
M-3.1a	O	2.07	19.39				
M-3.1b		2.07	20.16				
M-3.2a	O	1.96	23.43				
M-3.2b		1.93	24.97				
M-3.3a	R	2.08	21.83				
M-3.3b		1.99	24.46				
M-3.4a	O	2.07	16.01				
M-3.4b		2.02	17.49				
M-3.5a	R	2.01	22.19				
M-3.5b		2.11	19.51				
S-3.1a	O			Cylindrical/15 × 30	2	8.26	8.26
S-3.1b				Cubic/10 × 10 × 10	1	9.11	8.20
S-3.1c				Cubic/10 × 10 × 10	1	8.23	7.40
S-3.1d				Cylindrical/15 × 30	2	6.22	6.22
S-3.2a	O	1.93	25.21	Cubic/10 × 10 × 10	1	5.82	5.24
S-3.2b		2.04	19.72				
S-3.3a	O	1.86	29.17				
S-3.3b		1.84	30.29				
S-3.4	O			Cylindrical/15 × 30	2	4.65	4.65

[a] O, original rammed earth; R, rammed earth restored to one side.

depths greater than 30–35 cm, the lime was not fully carbonated, so the cores would not have reached the maximum mechanical strength. However, it should also be taken into account that the coring method could have altered the samples, as was seen in drillings soundings S-3.2 and S.3.3, whose inner parts were more damaged. However, some authors state that a high degree of carbonation is not a key factor in the properties of a lime mortar [68], so that the high mechanical properties of S-3.1 may rest on other physical characteristics such as bulk density or open porosity, which have not been possible to establish for this case.

In general terms, if the lime, grain size and physical properties are taken into account, it is possible to assert that these walls were properly manufactured and could be similar to lime concretes in terms of their physical characteristics.

5. Conclusions

The studies carried out allow to corroborate, and even deepen, one of the main characteristics of the monument today, the heterogeneity of the materials that make up the elements of the rammed earth wall.

- Among all the materials analysed, there are common mineralogical features, especially the presence of siliceous aggregates. In the grain size distributions, the high proportions of coarse aggregates and the lack of balance of the restitution materials stand out, especially in sectors 1 and 2.
- From a physical and mechanical aspect (bulk density, open porosity and compressive strength), there is a homogeneity among the original materials, characterized by a high bulk density (around 2 g/cm^3), low open porosity (many samples present values below 20%) and compressive strength in line with what other previous studies had established for this kind of walls (maximum 8–9 N/mm^2). In reference to these same aspects, the replacement materials present appreciably different values, especially with regard to open porosity, which is shown to be higher than in the originals.
- There are also differences in terms of the maximum lime contents determined. Although the original rammed earth walls are usually richer in lime than the replacement rammed earth, it is not possible to contrast whether it is also evident in terms of mechanical behaviour since there was not enough sample of the restored walls available.
- The grain size distribution, determining the degree of compaction of the aggregate, also affects the loss of cohesion of materials. Samples with grain size discontinuities or excess of fines or coarse grains produce more porous rammed earth which, therefore, are more susceptible to decohesion and loss of mass in the surface.
- It can be concluded that the dosage of the original rammed earth has a better aggregate gradient composition than the restored one. The rammed earth made for the restoration present a higher content of coarse aggregates and sands of larger diameter than those used in the original ones, which proves that more control was needed in the design of the compositions and the materials used in the restoration works and that they were corrected as the different phases of the wall execution progressed. This aspect is confirmed, as it has also been previously highlighted, through the results of the physical determinations, which establish a higher open porosity, which is symptomatic of a construction material of inferior execution quality
- The presence of soluble salts is high in general. The abundance of sulphates and chlorides stands out, although it is the former that can directly cause the most damage. The combination of capillary rising water and salts in these rammed earth walls is a good indicator of the

state of degradation. These salts, with a general predominance of sulphates, carried from the interior of the wall, are the ones that weaken the surface of the rammed earth and cause its gradual disintegration.

- It can be established that the main cause of the degradation of the wall is the loss of material and physical-chemical weathering. The cause does not lie in the material composition or poor performance of the original materials, but rather in the presence of water in the walls, its transport, and the crystallization of salts. This effect is worsened when the hygrothermal behaviour is altered, mainly by the existing excessive presence of water in the soil.

Therefore, the differences and parallels established constitute a set of basic characteristics to be taken into account for the study of new restoration materials, so that they do not alter the basic properties and physical-mechanical behaviour of existing materials. Furthermore, the analytical techniques employed, both destructive and non-destructive, provide important support for predictive maintenance and preventive conservation to help preserve the material values of the medieval wall of Seville.

CRediT authorship contribution statement

J.J. Martín-del-Rio: Conceptualization, Data curation, Formal analysis, Investigation, Methodology, Resources, Supervision, Validation, Writing – original draft. **J. Canivell:** Conceptualization, Data curation, Formal analysis, Investigation, Methodology, Resources, Supervision, Validation, Writing – original draft. **Marta Torres-González:** Conceptualization, Data curation, Formal analysis, Investigation, Methodology, Software, Supervision, Validation, Visualization, Writing – original draft, Writing – review & editing. **E.J. Mascort-Albea:** Resources, Supervision, Validation, Writing – review & editing. **R. Romero-Hernández:** Resources, Supervision, Validation, Writing – review & editing. **J.M. Alducin-Ochoa:** Data curation, Formal analysis, Investigation, Resources, Validation, Writing – review & editing. **F.J. Alejandre-Sánchez:** Funding acquisition, Investigation, Project administration, Resources, Supervision.

Declaration of competing interest

The authors declare that they have no known competing financial interests or personal relationships that could have appeared to influence the work reported in this paper.

Acknowledgements

This research has been developed within the framework of the "Specific collaboration agreement between the University of Sevilla and the Urban Planning Management of the Sevilla City Council, for the development of strategies aimed at the restoration and subsequent preventive conservation of the medieval wall of Sevilla". The authors express their gratitude to the Sevilla City Council's Urban Planning Department, especially the Urban Conservation and Building Renovation Service and the Urban Planning and Development Service. We would also like to thank the General Research Services of the University of Sevilla for their support in the tests carried out and the company Labrum S.A. for their collaboration and resources provided for the development of this research.

References

[1] C. Cacciavillani, S. Rinaldi, M. Severini, Vernacular construction techniques and earth employ in arg-e-bam (Iran), in: Vernacular and Earthen Architecture: Conservation and Sustainability - Proceedings of SOStierra2017 2017, CRC Press/Balkema, 2018, pp. 59–64, https://doi.org/10.1201/9781315267739-10.

[2] H. Schroeder, Sustainable Building with Earth, Springer International Publishing, Cham, 2016.

[3] F. Font, P. Hidalgo, Arquitecturas de tapia, Colegio Oficial de Aparejadores y Arquitectos Técnicos de Castellón, Castellón, 2009.

[4] G. Minke, Building with Earth: Design and Technology of a Sustainable Architecture, Birkhäuser, Basel etc., 2006.

[5] F.J. López Martínez, Tapias Y Tapiales, Loggia : Arquitectura Y Restauración, 1999, pp. 74–89, https://doi.org/10.4995/loggia.1999.5288.

[6] R. Azuar, Las técnicas constructivas en la formación de al-Andalus, Arqueología de La Arquitectura 4 (2005) 149–160.

[7] S. Márquez Bueno, P. Gurriarán Daza, Recursos formales y constructivos en la arquitectura militar almohade de al-Andalus, Arqueología de La Arquitectura 5 (2008) 115–134, https://doi.org/10.3989/arq.arqt.2008.92.

[8] J. López Osorio, The Nasrid ramparts of the Albaicín (Granada, Spain): an analysis of materials and building techniques, in: Vegas, Cristini (Eds.), Rammed Earth Conservation – Mileto, Taylor & Francis Group, London, 2012, ISBN 978-0-415-62125-0, pp. 27–32.

[9] S. Quesada-García, G. Romero-Vergara, El sistema de torres musulmanas en tapial de la Sierra de Segura (Jaén). Una contribución al estudio del mundo rural y el paisaje de al-Andalus, Arqueología de La Arquitectura, 2019, p. e079, https://doi.org/10.3989/arq.arqt.2019.001.

[10] S.M. Bueno, Constructive Technology of Al-Ándalus: Formwork and Coating in Military Architecture (XI-XIII Th). The Example of the Towers, Arqueologia de La Arquitectura, 2018, https://doi.org/10.3989/arq.arqt.2018.007 e076–e076.

[11] J. Canivell, A. Graciani, Latest trends in rammed earth restoration in western Andalucía, in: Earthen Architecture: Past, Present and Future - Proceedings of the International Conference on Vernacular Heritage, Sustainability and Earthen Architecture, CRC Press/Balkema, 2015, pp. 67–73.

[12] A. Graciani, M.Á. Tabales, El tapial en el área sevillana. Avance cronotipológico estructural, Arqueología de La Arquitectura 5 (2008) 135–158, https://doi.org/10.3989/arq.arqt.2008.93.

[13] F.J. Alejandre, J.J. Martín del Río, J. Blasco López, V. Flores, J.J. del Río, J. B. López, V. Flores, Methodological proposal for rammed-earth wall characterization: understanding of material in preliminary studies, in: Vegas, Cristini (Eds.), Rammed Earth Conservation – Mileto, Taylor & Francis Group, London, 2012, ISBN 978-0-415-62125-0, pp. 41–46.

[14] J.J. Martín-del-Rio, V. Flores-Alés, F.J. Alejandre-Sánchez, F.J. Blasco-López, New method for historic rammed-earth wall characterization: the almohade ramparts of Malaga and Seville, Stud. Conserv. (2018) 1–10, https://doi.org/10.1080/00393630.2018.1544429.

[15] E. Ontiveros-Ortega (Ed.), Programa de normalización de estudios previos aplicado a bienes inmuebles, Junta de Andalucia, Sevilla, 2006.

[16] J. Canivell, R. Rodríguez-García, A.M. González-Serrano, A. Romero Girón, Assessment of heritage rammed-earth buildings. The Alcázar of king Don Pedro I (Spain), J. Architect. Eng. (2020), https://doi.org/10.1061/(ASCE)AE.1943-5568.0000400.

[17] M. del M. Moreno Ruiz, P. Ortiz Calderón, R. Ortiz Calderón, Vulnerability study of earth walls in urban fortifications using cause-effect matrixes and GIS: the case of Seville, Carmona and Estepa defensive fences, Mediterr. Archaeol. Archaeometry 19 (2019) 119–138, https://doi.org/10.5281/zenodo.3583063.

[18] B. Medvey, G. Dobszay, Durability of stabilized earthen constructions: a review, Geotech. Geol. Eng. (2020) 1–23, https://doi.org/10.1007/s10706-020-01208-6.

[19] C.T.S. Beckett, C.E. Augarde, Development of Microstructure in Compacted Earthen Building Materials, Fifth International Conference on Unsaturated Soils, 2010, pp. 139–144.

[20] J. Canivell, E.J. Mascort-Albea, E. Cabrera-Revuelta, R. Romero-Hernández, A. Jaramillo-Morilla, Á. Serrano-Chacón, A methodological framework for the preventive conservation of historic walls located in urban contexts. Spatial data standards for the medieval wall of Seville (Spain): the case of the Macarena sector, Ge-Conservacion. 18 (2020) 44–55, https://doi.org/10.37558/gec.v18i1.762.

[21] A. Mellaikhafi, A. Tilioua, H. Souli, M. Garoum, M.A. Alaoui Hamdi, Characterization of different earthen construction materials in oasis of south-eastern Morocco (Errachidia Province), Case Stud. Construct. Mater. 14 (2021), e00496, https://doi.org/10.1016/j.cscm.2021.e00496.

[22] F. Bakadi, M. Rouai, A. Dekayir, E.M. Benyassine, Degradation Study of an Earthen Historical Rampart of Meknes City (Morocco) Using Ultrasonic Non-destructive Testing, Springer, Singapore, 2020, pp. 1267–1273, https://doi.org/10.1007/978-981-15-2184-3_167.

[23] I. Lombillo, L. Villegas, E. Fodde, C. Thomas, In situ mechanical investigation of rammed earth: calibration of minor destructive testing, Construct. Build. Mater. 51 (2014) 451–460, https://doi.org/10.1016/j.conbuildmat.2013.10.090.

[24] Y. Du, W. Chen, K. Cui, K. Zhang, W. Chen, Study on damage assessment of earthen sites of the ming great wall in Qinghai province based on study on damage assessment of earthen sites of the ming great wall in Qinghai province based on fuzzy-AHP and AHP-TOPSIS, Int. J. Architect. Herit. (2019) 1–14, https://doi.org/10.1080/15583058.2019.1576241, 0.

[25] E. Ontiveros-Ortega, E. Sebastián Pardo, I. Valverde Espinosa, Deterioration in XI-XIV century arab ramparts (Granada, Spain), Mater. Struct. 32 (1999) 45–51.

[26] M. Lanzón, V. De Stefano, J.C.M. Gaitán, I.B. Cardiel, M.L. Gutiérrez-Carrillo, Characterisation of earthen walls in the Generalife (Alhambra): microstructural and physical changes induced by deposition of Ca(OH)2 nanoparticles in original and reconstructed samples, Construct. Build. Mater. 232 (2020) 117202, https://doi.org/10.1016/J.CONBUILDMAT.2019.117202.

[27] M.L. Gutierrez-Carrillo, A. Arizzi, I. Bestué Cardiel, E. Sebastián Pardo, Study of the state of conservation and the building materials used in defensive constructions in south-eastern Spain: the example of Mula Castle in Murcia, Int. J. Architect. Herit. (2019) 1–13, https://doi.org/10.1080/15583058.2019.1630516.

[28] J.L. Parracha, A.S. Silva, M. Cotrim, P. Faria, Mineralogical and microstructural characterisation of rammed earth and earthen mortars from 12th century Paderne Castle, J. Cult. Herit. 42 (2020) 226–239, https://doi.org/10.1016/j.culher.2019.07.021.
[29] M.I. Mota-lópez, R. Maderuelo-Sanz, J.D. Pastor-valle, J.M. Meneses-rodríguez, A. Romero-casado, Analytical characterization of the almohad rammed-earth wall of Cáceres, Spain, Construct. Build. Mater. 273 (2021) 1216763, https://doi.org/10.1016/j.conbuildmat.2020.121676.
[30] C. Mileto, F. Vegas, F.J. Alejandre, J.J. Martín, L.G. Soriano, L. García Soriano, Lime-crusted rammed earth: materials study, Adv. Mater. Res. 831 (2014) 9–13. https://doi.org/10.4028/www.scientific.net/AMR.831.9.
[31] A. Graciani, J.J. Martín del Río, G.M. Mora, F.J. Alejandre, J. Canivell, Preliminary Studies for Intervention, Interpretation and Value Enhancement of Tower of Don Fadrique (Albaida, Seville, Spain), in: Rammed Earth Conservation, Taylor & Francis Group, London, 2012, pp. 345–350.
[32] F.J. Blasco-López, J. Canivell, A. Graciani, J.J. Martin-del-Río, F.J. Alejandre, The Keep of the Alcázar of Carmona (Sevilla, Spain). Materials for the Restoration of Rammed Earth Walls, in: Vernacular and Earthen Architecture: Conservation and Sustainability, Taylor & Francis Group, 2017, https://doi.org/10.1201/9781315267739.
[33] F.J. Alejandre, J.J. Martín del Río, J.J. del Río, Caracterización analítica de la Muralla de Tapial almohade de San Juan de Aznalfarache, in: Construir Con Tierra Ayer y Hoy. V Siacot. Seminario Iberoamericano de Construcción Con Tierra y I Seminario Argentino de Arquitectura y Construcción Con Tierra (5), vol. 5, Zeta Editores, Srl, 2006, pp. 119–120.
[34] Á. Barrios Padura, A. Graciani, L. Núñez, Á.B. Padura, A. Graciani, L. Núñez, Characterization of the rammed-earth structure of the Moon Castle in Mairena del Alcor (Seville, Spain), in: Rammed Earth Conservation, Taylor & Francis Group, London, 2012, pp. 263–267.
[35] J.J. Martín-del-Rio, F.J. Alejandre, F.J. Blasco-López, G. Márquez Martínez, Hormigones de cal islámicos: altas resistencias en los tapiales del sector oriental de la Muralla de Sevilla (España), in: Actas de IX CICOP 2008. Congreso Internacional de Rehabilitación Del Patrimonio Arquitectónico y Edificación. Patrimonio Construido e Innovación., Centro Internacional de Conservación del Patrimonio, vol. I, CICOP, Gran Canaria, 2008, pp. 81–86.
[36] Á.R. Serrano-Chacón, E.J. Mascort-Albea, J. Canivell, R. Romero-Hernández, A. Jaramillo-Morilla, Multi-criteria parametric verifications for stability diagnosis of rammed-earth historic urban ramparts working as retaining walls, Appl. Sci. 11 (2021) 2744, https://doi.org/10.3390/app11062744.
[37] G. Carapellese, J. Canivell, J.J. Martín-Del-Río, A. Graciani-García, E. Cabrera-Revuelta, Evaluación de fortificaciones rurales de tapia mediante técnica SfM de fotogrametría digital. Aplicación metodológica al Castillo de Alhonoz (Écija, España), Estoa 9 (2020) undefined–113, https://doi.org/10.18537/est.v009.n018.a09.
[38] E. Diz-Mellado, E.J. Mascort-Albea, R. Romero-Hernández, C. Galán-Marín, C. Rivera-Gómez, J. Ruiz-Jaramillo, A. Jaramillo-Morilla, Non-destructive testing and Finite Element Method integrated procedure for heritage diagnosis: the Seville Cathedral case study, J. Build. Eng. 37 (2021) 102134, https://doi.org/10.1016/j.jobe.2020.102134.
[39] D. Jiménez Maqueda, P. Pérez Quesada, La muralla huérfana. A vueltas con el último recinto amurallado de Madnat Isblia, Romula 12 (2012) 273–347.
[40] J. García-Tapial, J.M. Cabeza Méndez, Restauración de la Murallas de la Macarena, Aparejadores: Boletín del Colegio Oficial de Aparejadores, y Arquitectos Técnicos de Sevilla 20 (1986) 9–17.
[41] J.M. Cabeza Méndez, Restauración de la murallas de Sevilla, in: Arquitectura y Ciudad II y III : Seminarios Celebrados En Melilla, Los Días 25, 26 y 27 de Septiembre de 1990 y Los Días 24, 25 y 26 de Septiembre de 1991, Instituto de Conservación y Restauración de Bienes Culturales, Madrid, 1993, pp. 341–348.
[42] J. García-Tapial, J.M. Cabeza Méndez, Recuperación de la cerca almohade de la ciudad de Sevilla en el recinto de la Casa de la Moneda, Archivo Hispalense 72 (1989) 291–297.
[43] J. García-Tapial, J.M. Cabeza Méndez, Restauración de las murallas del Jardín del Valle, Aparejadores: Boletín Del Colegio Oficial de Aparejadores y Arquitectos, Técnicos de Sevilla 26 (1988) 26–31.
[44] A. Graciani, J. Canivell, Revisión de las Intervenciones en Fábricas de Tapia en Andalucía Occidental, in: F. Mileto, C. Vegas (Eds.), Restauración de La Tapia En La Península Ibérica. Criterios, Técnicas, Resultados, Perspectivas, General de Ediciones de Arquitectura, 2014, pp. 30–41.
[45] U.R. and C.S. of the S.C. Council, Project for the Restoration and Consolidation of the Macarena's Rampart, 2019.
[46] F. Champiré, A. Fabbri, J.C. Morel, H. Wong, F. McGregor, Impact of relative humidity on the mechanical behavior of compacted earth as a building material, Contruct. Build. Mater. 110 (2016) 70–78, https://doi.org/10.1016/j.conbuildmat.2016.01.027.
[47] Q.B. Bui, J.C. Morel, B.V.V. Reddy, W. Ghayad, B.V. Venkatarama Reddy, W. Ghayad, Durability of rammed earth walls exposed for 20 years to natural weathering, Build. Enviroment 44 (issue) (2009) 912–919.
[48] Y. Shen, W. Chen, J. Kuang, W. Du, Effect of salts on earthen materials deterioration after humidity cycling, J. Cent. S. Univ. 24 (2017) 796–806, https://doi.org/10.1007/s11771-017-3482-0.
[49] AENOR, UNE-EN 772-5:2016. Methods of Test for Masonry Units - Part 5: Determination of the Active Soluble Salts Content of Clay Masonry units., Spain, 2016.
[50] AENOR, UNE-EN ISO 17892-4:2019. Particle Size Analysis of a Fine Soil by Sedimentation, Densimeter method., Spain, 2019.
[51] AENOR, UNE-EN 1936-07:2007. Natural Stone Test Methods - Determination of Real Density and Apparent Density, and of Total and Open porosity., Spain, 2007.
[52] P. Walker, The Australian Earth Building Handbook, Standards Australia International, Sydney, Australia, 2001. http://fama.us.es/record=b2667501~S5*spi. (Accessed 6 October 2015).
[53] AENOR, UNE-EN 12504-1:2020. Testing Concrete in Structures. Part 1: Cored Specimens. Taking, Examining and Testing in compression., Spain, 2020.
[54] AENOR, UNE-EN 1015-11. Methods of Test for Mortar for Masonry - Part 11: Determination of Flexural and Compressive Strength of Hardened mortar., Spain, 2000.
[55] P. Walker, HB 195. The Autralian Earth Builing Handbook, 2002.
[56] M.I. González Díez, Estudio geológico del área urbana de Sevilla y alrededores, Universidad de Sevilla, 1986.
[57] D. Ciancio, C.T.S. Beckett, J.A.H. Carraro, Optimum lime content identification for lime-stabilised rammed earth, Construct. Build. Mater. 53 (2014) 59–65, https://doi.org/10.1016/j.conbuildmat.2013.11.077.
[58] E. Ontiveros-Ortega, E. Sebastian Pardo, I. Valverde-Espinosa, F.J. Gallego Roca, Estudio de los materiales de construcción de las murallas del Albayzín (Granada), PH, vol. 66, Boletín Del Instituto Andaluz Del Patrimonio Histórico, 2008, pp. 32–47.
[59] A. Arnold, A. Kung, K. Zehnder, Deterioration and preservation of Carolingian and mediaeval mural paintings in the Müstair Convent (Switzerland) Part I: Decay mechanisms and preservation, Stud. Conserv. 31 (1986) 190–194, https://doi.org/10.1179/sic.1986.31.Supplement-1.190.
[60] N. Proietti, P. Calicchia, F. Colao, S. De Simone, V. Di Tullio, L. Luvidi, F. Prestileo, M. Romani, A. Tatì, Moisture damage in ancient Masonry: a multidisciplinary approach for in situ Diagnostics, Minerals 11 (2021) 406, https://doi.org/10.3390/MIN11040406, 11 (2021) 406.
[61] K. Cui, Y. Du, Y. Zhang, G. Wu, L. Yu, An evaluation system for the development of scaling off at earthen sites in arid areas in NW China, Heritage Science 7 (2019) 14, https://doi.org/10.1186/s40494-019-0256-z.
[62] M. Shao, L. Li, S. Wang, E. Wang, Z. Li, Deterioration mechanisms of building materials of Jiaohe ruins in China, J. Cult. Herit. 14 (2013) 38–44, https://doi.org/10.1016/j.culher.2012.03.006.
[63] J. Martínez-Martínez, E. Torrero, D. Sanz, V. Navarro, Salt crystallization dynamics in indoor environments: stone weathering in the Muñoz Chapel of the Cathedral of Santa María (Cuenca, central Spain), J. Cult. Herit. 47 (2021) 123–132, https://doi.org/10.1016/j.culher.2020.09.011.
[64] A. Arnold, K. Zehnder, Monitoring wall paintings affected by soluble salts Conservation of wall paintings View project, in: Sharon Carther (Ed.), The Conservation of Wall Paintings, Getty Conservation Institute, London, 1987, pp. 103–135.
[65] H. Houben, H. Guillaud, Earth Construction: a Comprehensive Guide, Intermediate Technology Development Group, London, UK, 2008.
[66] J. Canivell, J.J. Martin-del-Rio, F.J. Alejandre, J. García-Heras, A. Jimenez-Aguilar, Considerations on the physical and mechanical properties of lime-stabilized rammed earth walls and their evaluation by ultrasonic pulse velocity testing, Construct. Build. Mater. 191 (2018) 826–836, https://doi.org/10.1016/J.CONBUILDMAT.2018.09.207.
[67] Q.B. Bui, J.C. Morel, Assessing the anisotropy of rammed earth, Construct. Build. Mater. 23 (2009) 3005–3011, https://doi.org/10.1016/j.conbuildmat.2009.04.011.
[68] E. Ontiveros-Ortega, R. Rodríguez-García, A. González-Serrano, L. Molina, Evolution of mechanical properties in aerial lime mortars of traditional manufacturing, the relationship between putty and powder lime, Construct. Build. Mater. 191 (2018) 575–589, https://doi.org/10.1016/J.CONBUILDMAT.2018.10.053.